

SYNCHRONIZATION OF MECHANICAL OSCILLATORS EXCITED KINEMATICALLY

PRZEMYSŁAW PERLIKOWSKI

Technical University of Lodz, Division of Dynamics, Lodz, Poland

e-mail: przemyslaw.perlikowski@p.lodz.pl

In this paper, the behaviour of a system of coupled mechanical oscillators excited kinematically was studied numerically. Several methods of detection of synchronization were shown and advantages of each were mentioned. The relation between Lyapunov exponents and the synchronization state under different kinds of the excitation signal (harmonic, periodic and chaotic ones) was presented. It was demonstrated that the mode locking with excitation was dependent only on inner damping and completely uncorrelated with the connection between oscillators.

Key words: synchronization, mechanical oscillators, kinematic excitation

1. Introduction

The phenomenon of synchronization in dynamics has been known for a long time. Recently, the idea of synchronization has been also adopted for non-linear systems. It has been demonstrated that two or more non-linear systems can be synchronized by linking them with mutual coupling or with a common signal or signals (Blekhman *et al.*, 1995; Boccaletti *et al.*, 2002; Kapitaniak, 1994; Pecora and Carroll, 1990; Pyragas, 1993). In the case of linking, a set of identical chaotic systems (the same set of ODEs and values of the system parameters) Complete Synchronization (CS) can be obtained. The complete synchronization takes place when all trajectories converge to the same value and remain in step with each other during further evolution (i.e. $\lim_{t \rightarrow \infty} |x(t) - y(t)| = 0$ for two arbitrarily chosen trajectories $x(t)$ and $y(t)$). In such a situation, all subsystems of the augmented system evolve on the same invariant manifold on which one of these subsystems evolves (the phase space is reduced to the synchronization manifold). The linking of homochaotic systems (i.e.

systems given by the same set of ODEs but with different values of the system parameters) can lead to Imperfect Complete Synchronization (ICS) (i.e. $\lim_{t \rightarrow \infty} |x(t) - y(t)| \leq \varepsilon$, where ε is a vector of small parameters) (Kapitaniak *et al.*, 1996). A significant change of the chaotic behaviour of one or more systems can be also observed in such linked systems. This so-called "controlling chaos by chaos" procedure has some potential importance for mechanical and electrical systems. An attractor of such two systems coupled by a negative feedback mechanism can be even reduced to the fixed point (Stefański and Kapitaniak, 1996).

Recently, another type of synchronization has been detected in non-linear systems called Phase Synchronization (PS) (Rosenblum *et al.*, 1996; Rosenblum *et al.*, 2001). It can be introduced as synchronization of periodic oscillators, where only the phase locking is necessary, while no requirements on the amplitudes is imposed. The PS in non-linear systems is defined as the appearance of reaction between phases of subsystems (or between the phase of subsystems and the driving signal), while the amplitudes can still be non-linear and non-correlated.

From the viewpoint of practical considerations, a periodic and non-periodic excitation can be met in mechanical systems. For that reason, this paper is concentrated on analysis of the CS of a set of identical mechanical oscillators linked by a common excitation. Interactions between phases of the excitation and oscillators were taken under consideration. The presented analysis is based on connections between the appearance of synchronization and Lyapunov Exponents (LEs), and it is motivated by Pecora and Carroll's theoretical and experimental studies (Pecora and Carroll, 1990, 1991). It has been discovered that uncoupled non-linear systems linked by common signals can synchronize if LEs for the subsystems reaches negatives values. In the next paper by Pecora and Carroll (1998) a concept called Master Stability Function (MSF) was introduced. It has been proved that the system of coupled non-linear oscillators can synchronize when all Transversal Lyapunov Exponents (TLEs) are negative. Considerations presented in this paper, which are supported by numerical analysis, shown that even a non-periodic nature of common external excitation can lead to synchronization of driven mechanical oscillators. The necessary, but not sufficient, condition for the occurrence of synchronization is the negative sign of LEs associated with the response of the system. In the numerical experiment, a pair of non-linear mechanical oscillators of the Duffing type, coupled or uncoupled, forced by different types of excitation has been used. All numerical simulations have been carried out with programs written in C++, and for calculating LEs and TLEs algorithms by Parker and

Chua (1989) have been used. The paper is organized as follows. In Sec. 2 some theoretical fundamentals are recalled. Section 3 describes types of oscillators which are used in numerical investigations. Section 4 is devoted to numerical examples. A brief conclusion is presented in Sec. 5.

2. Complete synchronization, phase synchronization and Lyapunov exponents

2.1. Complete synchronization of uncoupled systems

Consider a set of l separate identical j -degree-of-freedom mechanical oscillators forced by a common signal as shown in Figure 1. The character of excitation (function $e(t)$) and differential equations describing the motion of oscillators can be chosen arbitrarily. The dynamical state each of these oscillators is determined by the j -dimensional vector $\mathbf{x}_i = [x_{i1}, x_{i2}, \dots, x_{ij}]$, ($i = 1, 2, \dots, l$). This vector describes a response generated by the system. The r -dimensional vector $\mathbf{e} = [e_1, e_2, \dots, e_r]$ describes evolution of the excitation. Thus, the state of a separate subsystem is described in the phase space of $h = j + r$ dimension, and the equations of motion of such a subsystem can be written in a general first order differential equation autonomous form

$$\dot{\mathbf{x}}_i = f(\mathbf{x}_i, \mathbf{e}) \quad \dot{\mathbf{e}} = f(\mathbf{e}) \tag{2.1}$$

where $\mathbf{x}_i \in \mathbb{R}^j$ ($i = 1, 2, \dots, l$) and $\mathbf{e} \in \mathbb{R}^r$.

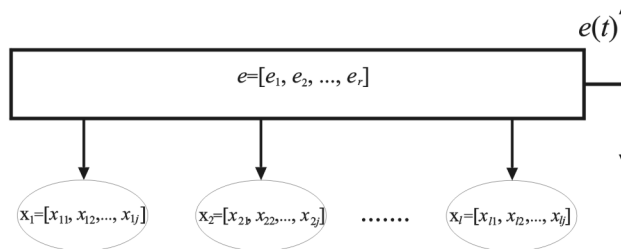


Fig. 1. The scheme of the system under consideration

Equation (2.1) describes the dynamical evolution of excitation in the s -dimensional subspace of the system phase space (*excitation subspace*). From the form of Eqs. (2.1) it results that the time evolution of excitation is independent of the remaining state variables and is characterized by Lyapunov exponents, where at least one of them is equal to zero. Equation (2.1)₁ describes

the evolution of the system response (*response subspace*) in the j -dimensional subspace of the phase space which is transversal to the above mentioned *excitation subspace* and is characterized by a series of j LEs. A two-dimensional visualization of the system phase space is presented in Fig. 2. This idea was proposed by Stefański and Kapitaniak (2003b).

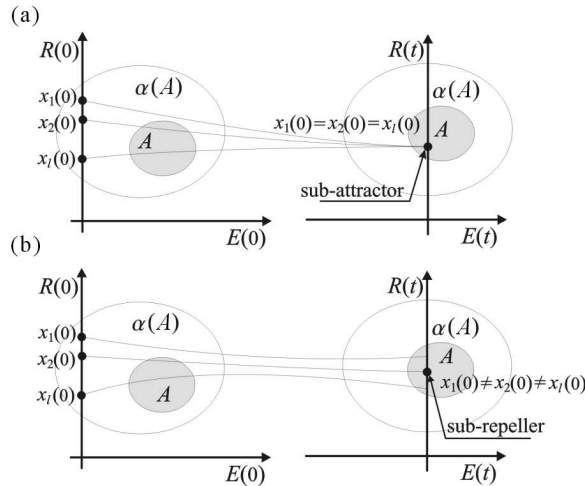


Fig. 2. Two-dimensional visualization of synchronization (a) and desynchronization (b); attractor of the chaotic system; $\alpha(A)$ basin of attraction of the attractor A ; E excitation subspace; R response subspace

The common excitation causes that the distance between trajectories in the direction associated with zero LE amounts to zero and the trajectories can be found in the same j -dimensional *response subspace* at each moment. This fact leads to the conclusion that for a set of negative RLEs there exists a point in the *response subspace* which is a stable *sub-attractor*. This point is a trace of the system attractor in the *response subspace*. If the trajectories start from different points of the basin of attraction, then they evolve to the same state and the oscillators will synchronize (Fig. 2a). In other words, an invariant subspace representing the synchronized state ($\mathbf{x}_1 = \mathbf{x}_2 = \dots = \mathbf{x}_l$) is a stable attractor. Such synchronization is caused by the common excitation only, and it occurs without any additional coupling between the oscillators.

If at least one RLEs is positive, then the synchronization between the oscillators under consideration is impossible. It means that instability associated with positive RLEs causes divergence of nearby trajectories (Fig. 2b) in the *response subspace*, and the *sub-attractor* becomes a *sub-repeller* representing an unstable orbit in this subspace.

2.2. Complete synchronization of coupled systems

Systems with couplings between oscillators can not be treated in the same way as uncoupled ones. It is impossible to describe their behaviour as a system composed of independent oscillators. The idea of RLEs is not sufficient to determine synchronization. Different criteria have to be applied. Pecora and Carroll (1998) introduced a concept called the Master Stability Function, which allows one to determine the stability of synchronization by means of TLEs. The stability problem in this idea can be formulated in a very general way by addressing the question of stability of the CS manifold $\mathbf{x}_1 \equiv \mathbf{x}_2 \equiv \dots \equiv \mathbf{x}_i$. The CS exists when the synchronization manifold is asymptotically stable for all possible trajectories.

Considering a dynamical uncoupled system given by equations

$$\dot{\mathbf{x}}_i = f(\mathbf{x}_i) \quad (2.2)$$

$H : \mathbb{R}^m \rightarrow mIR^m$ is the output function of each oscillator variables that is used in the coupling, $\mathbf{x} = (\mathbf{x}_1, \mathbf{x}_2, \dots, \mathbf{x}_N) \in \mathbb{R}^m$, $\mathbf{F}(\mathbf{x}) = (f(\mathbf{x}_1), \dots, f(\mathbf{x}_N))$, \mathbf{G} is the matrix of coupling coefficients and σ is the coupling strength. An arbitrary set of N coupled (linear coupling) identical systems can be created

$$\dot{\mathbf{x}} = \mathbf{F}(\mathbf{x}_i) + (\sigma \mathbf{G} \otimes \mathbf{H}) \quad (2.3)$$

where \otimes is the direct (Kronecker) product. In this place, it should be recalled that the direct product of two matrices \mathbf{A} and \mathbf{B} is given by

$$\mathbf{A} \otimes \mathbf{B} = [a_{ij} \mathbf{B}] \quad (2.4)$$

where a_{ij} are elements of the matrix \mathbf{A} . Note also that the manifold invariant requires $\sum_j G_{ij} = 0$. The variational equation of Eq. (2.3) is

$$\dot{\varphi} = [\mathbf{I}_N \otimes \mathbf{DF} + \sigma \mathbf{G} \otimes \mathbf{DH}] \varphi \quad (2.5)$$

where $\varphi = (\varphi^1, \varphi^2, \dots, \varphi^N)$ are perturbations and \mathbf{I}_N is the $(N \times N)$ -dimensional identity matrix. After diagonalization, each block has the form

$$\dot{\varphi}_k = [\mathbf{DF} + \sigma \gamma_k \mathbf{DH}] \varphi_k \quad (2.6)$$

where γ_k is the eigenvalue of the connectivity matrix \mathbf{G} , ($k = 0, 1, 2, \dots, N - 1$). For $k = 0 \rightarrow \gamma_0$, one gets variational equation for the synchronization manifold. All k correspond to transverse eigenvectors, so one has succeed in separating the synchronization manifold from the other, transverse directions.

The Jacobian functions **DF** and **DH** are the same for each block, since they are evaluated on the synchronized state. Thus, for each k , the form of each block (Eq. (2.6)) is the same only with only the scalar multiplier $\sigma\gamma_k$ different for each of them. This leads to the following formulation of the master stability equation and the associated MSF. One can calculate the maximum TLE λ_1 for the generic variational equation

$$\dot{\varphi}_k = [\mathbf{DF} + (\delta + i\beta)\mathbf{DH}]\varphi_k \quad (2.7)$$

where $\sigma\gamma_k = \delta + i\beta$. In mechanical systems, we have mutual interaction, hence $\sigma\gamma_k = \delta$ (real coupling $\beta = 0$).

2.3. Phase synchronization

In chaotic oscillators, there is no unique phase of oscillations. The idea introduced by Rosenblum *et al.* (Rosenblum *et al.*, 1996, 2001) was applied to detect the phase. It enabled one to detect the PS between the oscillators and the driven signal. The amplitude and the phase of an arbitrary signal $s(t)$ has to be determined. A general approach was introduced by Gabor (1946) and it was based on the analytic signal concept by Rosenblum *et al.* (1996). The analytic signal $x(t)$ is a complex function of time defined as

$$x(t) = s(t) + j\tilde{s} = A(t)e^{j\phi(t)} \quad (2.8)$$

where the function $\tilde{s}(t)$ is the Hilbert transform of $s(t)$

$$\tilde{s} = \frac{1}{\pi} \text{P.V.} \int_{-\infty}^{\infty} \frac{s(\tau)}{t - \tau} d\tau \quad (2.9)$$

(where P.V. means that the integral is taken in the sense of the Cauchy principal value). The instantaneous amplitude $A(t)$ and the instantaneous phase $\phi(t)$ of the signal $s(t)$ are thus uniquely defined by equation (2.8). From (2.9), the Hilbert transform $\tilde{s}(t)$ of $s(t)$ may be considered as the convolution of the functions $s(t)$ and t/π . Hence, the Fourier transform $\tilde{S}(j\omega)$ of $\tilde{s}(t)$ is the product of the Fourier transforms of $s(t)$ and t/π . For physically relevant frequencies $\omega > 0$, $\tilde{S}(j\omega) = -jS(j\omega)$; i.e. ideally, $\tilde{s}(t)$ may be obtained from $s(t)$ by a filter whose amplitude response is unity, and whose phase response is a constant $\pi/2$ lag at all frequencies.

3. Duffing oscillator

The Duffing system has been chosen to present an example of a mechanical oscillator. The considered system is excited kinematically, what was shown in Fig. 3. Its evolution is described by

$$m\ddot{y} - d_y[\dot{e}(t) - \dot{y}] + k_y[e(t) - y] - k_d[e(t) - y]^3 = 0 \quad (3.1)$$

where m , d_y , k_y , k_d are viscous damping, linear and non-linear parts of stiffness of the spring, respectively, and $e(t)$ is the signal of excitation.

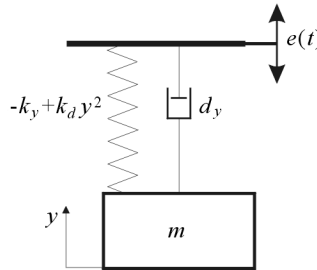


Fig. 3. Duffing oscillator

After introducing dimensionless variables, the following form of the equation of motion is obtained

$$\ddot{\xi} - c_1[\dot{c}_4(\tau) - \dot{\xi}] + [c_4(\tau) - \xi] - c_2[c_4(\tau) - \xi]^3 = 0 \quad (3.2)$$

where

$$\begin{aligned} \omega &= \frac{k_y}{m} & c_1 &= \frac{d_y}{m\omega} & c_2 &= \frac{k_d m y_{st}^2}{\omega^2 k_y^2} \\ c_4(\tau) &= \frac{e(t)}{y_{st}} & \dot{c}_4(\tau) &= \frac{\dot{e}(t)}{y_{st}\omega} & y_{st} &= \frac{mg}{k_y} \end{aligned}$$

In numerical analysis it is assumed that $c_2 = 2.0$. The inner damping c_1 is chosen as a controlling parameter. The excitation signal $c_4(\tau)$ depends on the type of excitation transmitted to the oscillator. It is described in Sec. 4 in more detail.

3.1. Two Duffing oscillators excited by common signal

A system of two Duffing oscillators excited by a common signal $e(t)$ is shown in Fig. 4.

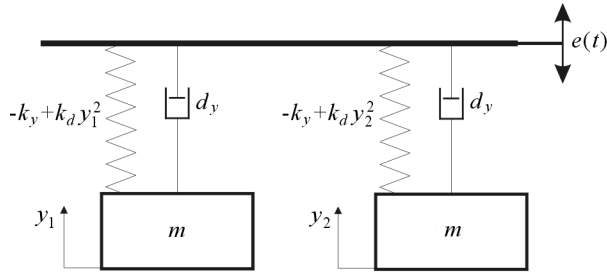


Fig. 4. Two Duffing oscillators with common excitation

This is the simplest example of the system given by Eqs. (??). According to Eqs. (3.2), the system shown in Fig. 4 can be described by the following dimensionless equations

$$\begin{aligned} \ddot{\xi}_1 - c_1[\dot{c}_4(\tau) - \dot{\xi}_1] + [c_4(\tau) - \xi_1] - c_2[c_4(\tau) - \xi_1]^3 &= 0 \\ \ddot{\xi}_2 - c_1[\dot{c}_4(\tau) - \dot{\xi}_2] + [c_4(\tau) - \xi_2] - c_2[c_4(\tau) - \xi_2]^3 &= 0 \end{aligned} \tag{3.3}$$

Common dynamics is realized by the kinematic excitation applied to the rigid suspension of oscillators, which ensures the same amplitude and phase of forcing.

3.2. Two dissipatively coupled Duffing oscillators excited by common signal

The system of two coupled Duffing oscillators excited by the common signal is taken under consideration. Due to mutual coupling, there are interactions between subsystems.

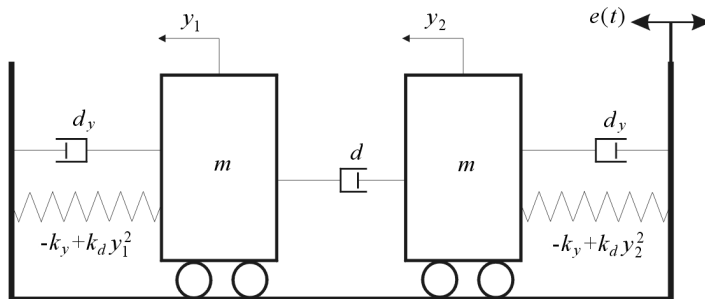


Fig. 5. Two coupled Duffing with common excitation

This system is a generalisation of the previous problem. When d_1 is equal to zero the system given by Eq. (3.3) is obtained. Motion of the system is given by dimensionless equations

$$\begin{aligned} \ddot{\xi}_1 - c_1[\dot{c}_4(\tau) - \dot{\xi}_1] + [c_4(\tau) - \xi_1] - c_2[c_4(\tau) - \xi_1]^3 + d_1[\dot{\xi}_1 - \dot{\xi}_2] &= 0 \\ \ddot{\xi}_1 - c_1[\dot{c}_4(\tau) - \dot{\xi}_1] + [c_4(\tau) - \xi_1] - c_2[c_4(\tau) - \xi_1]^3 - d_1[\dot{\xi}_1 - \dot{\xi}_2] &= 0 \end{aligned} \tag{3.4}$$

where: $d_1 = d/(m\omega)$ and $\omega, c_1, c_2, c_4(\tau), \dot{c}_4(\tau)$ are the same as in Eq. (3.2).

4. Numerical examples

4.1. Harmonic excitation

To show the idea of RLE on the simplest example, the harmonic excitation is applied to the Duffing oscillators. The excitation signal $e(t)$ is given by the equation $e(t) = a \sin(\Omega t)$. Hence, for the whole system, the dimensionless equations of motion are as follows

$$\begin{aligned} \ddot{\xi}_1 - c_1[\dot{c}_4(\tau) - \dot{\xi}_1] + [c_4(\tau) - \xi_1] - c_2[c_4(\tau) - \xi_1]^3 &= 0 \\ \ddot{\xi}_2 - c_1[\dot{c}_4(\tau) - \dot{\xi}_2] + [c_4(\tau) - \xi_2] - c_2[c_4(\tau) - \xi_2]^3 &= 0 \end{aligned} \tag{4.1}$$

where

$$\begin{aligned} c_4(\tau) &= \frac{a}{y_{st}} \sin(\eta\tau) & \dot{c}_4(\tau) &= \frac{a}{y_{st}} \eta \cos(\eta\tau) \\ \tau = \omega t & & \eta = \frac{\Omega}{\omega} &= 1 \end{aligned}$$

other parameters are the same as in the Eq. (3.2). As it was mentioned before, the controlling parameter is the dimensionless viscous damping c_1 . As can be seen in Figs. 6 and 7, there is a wide range of chaotic behaviour. It is well known that due to sensitivity to the initial condition, it is impossible to synchronize systems working in the chaotic regime without additional coupling between them. In Figs. 6 and 7, bifurcation diagrams of ξ_1 and the difference $\xi_1 - \xi_2$ as a function of c_1 are shown. As can be, the seen subsystems reach synchronization in ranges where a single oscillator has periodic behaviour. For each subsystem, there is a boundary value of c_1 after which the state of synchronization is stable and unchangeable despite an increase of c_1 . For the system with the amplitude of excitation $c_4(\tau) = 1.9 \sin \tau$ (Fig. 6) the boundary value is $c_1 = 0.2$, and for $c_4(\tau) = 2.2 \sin \tau$ (Fig. 7) is $c_1 = 0.27$. In

the second example, it is worth mentioning that "synchronization windows" in which synchronization appears exist between two ranges of desynchronization. Such a type of synchronization has been also detected in networks of coupled oscillators and has been called *Ragged Synchronizability* (RSA) (Stefański *et al.*, 2007).

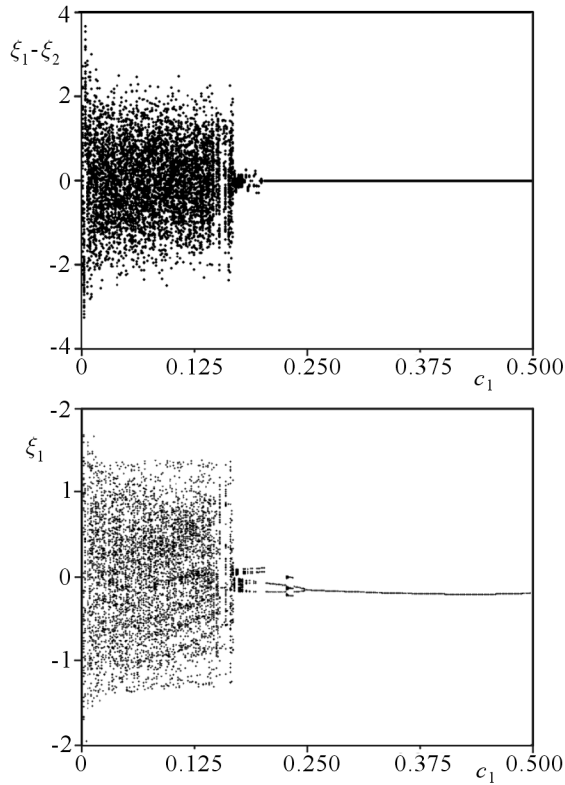


Fig. 6. Bifurcation diagram of a single oscillator excited by the periodic signal Eq. (4.1). Parameters: $c_1 \in (0.0, 0.5)$, $c_4(\tau) = 1.9 \cos \tau$

4.2. Non-linear excitation

In this Section, the system with the excitation signal given by a non-linear signal is taken under consideration. As a system generating non-linear forcing, the Duffing oscillator has been chosen. It is described by the dimensionless equation

$$\ddot{\beta} + 0.1\dot{\beta} - \beta + \beta^3 = q \sin \tau \quad (4.2)$$

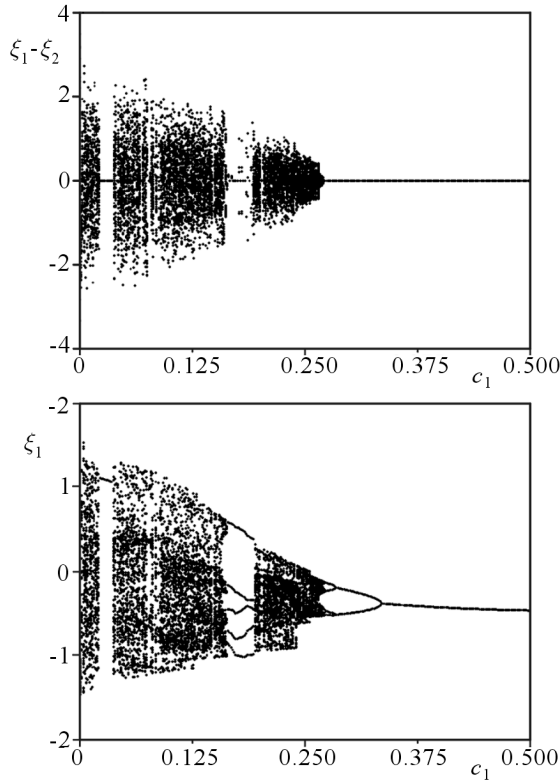


Fig. 7. Bifurcation diagram of a single oscillator excited by the periodic signal Eq. (4.1). Parameters: $c_1 \in (0.0, 0.5)$, $c_4(\tau) = 2.2 \cos \tau$

In this case, the investigated system is excited using a signal given by the variables β and $\dot{\beta}$, i.e. $c_4(\tau) = \beta$ and $\dot{c}_4(\tau) = \dot{\beta}$. For numerical simulations, three different values of the forcing amplitude are chosen:

1. $q = 4.0$ – periodic motion with the period one (Fig. 8)
2. $q = 5.6$ – chaotic motion (Fig. 9)
3. $q = 5.8$ – periodic motion with the period three (Fig. 10).

In Figures 8-10, three bifurcation diagrams depicting the relation between the controlling parameter c_1 versus $\xi_1 - \xi_2$, ξ_1 and Lyapunov exponents of the single subsystem (two RLEs and two ELEs) are presented respectively. In Sec. 2, the rule that the system reaches synchronization when RLEs reaches negative values is introduced. Thus, it is sufficient to calculate LEs for one subsystem only (in the case when subsystems are identical). It is worth to mention that the subsystems tend to behave like the excitation. For the periodic excitation with the period one, the oscillators reach period one motion and

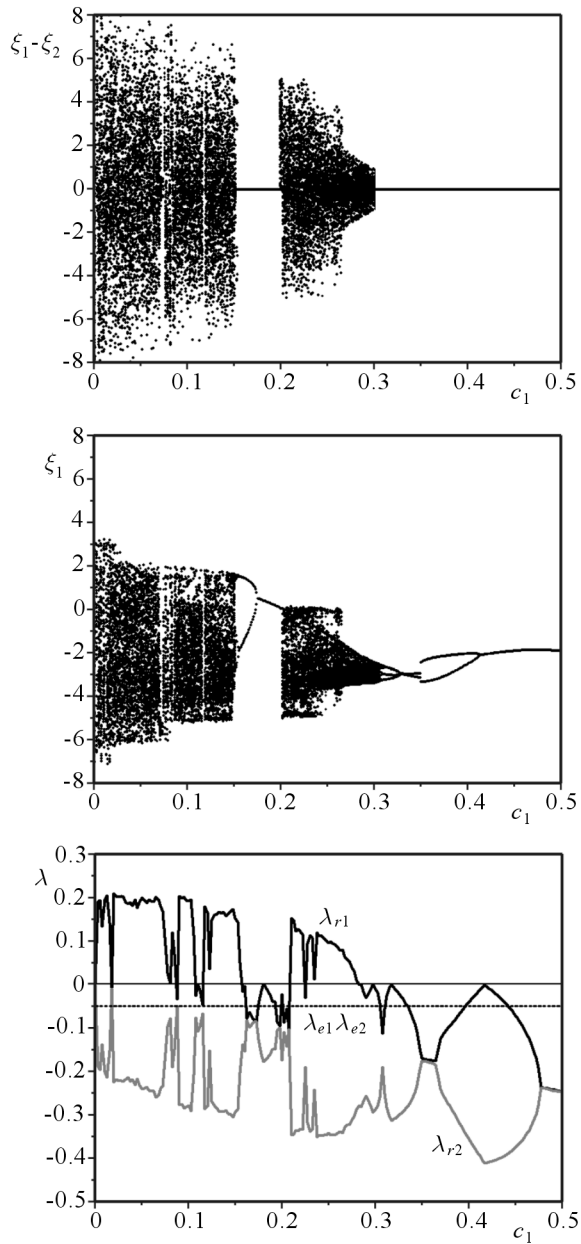


Fig. 8. Non-linear excitation – period one ($q = 4.0$), bifurcation diagrams of $\xi_1 - \xi_2$, ξ_1 and Lyapunov exponents

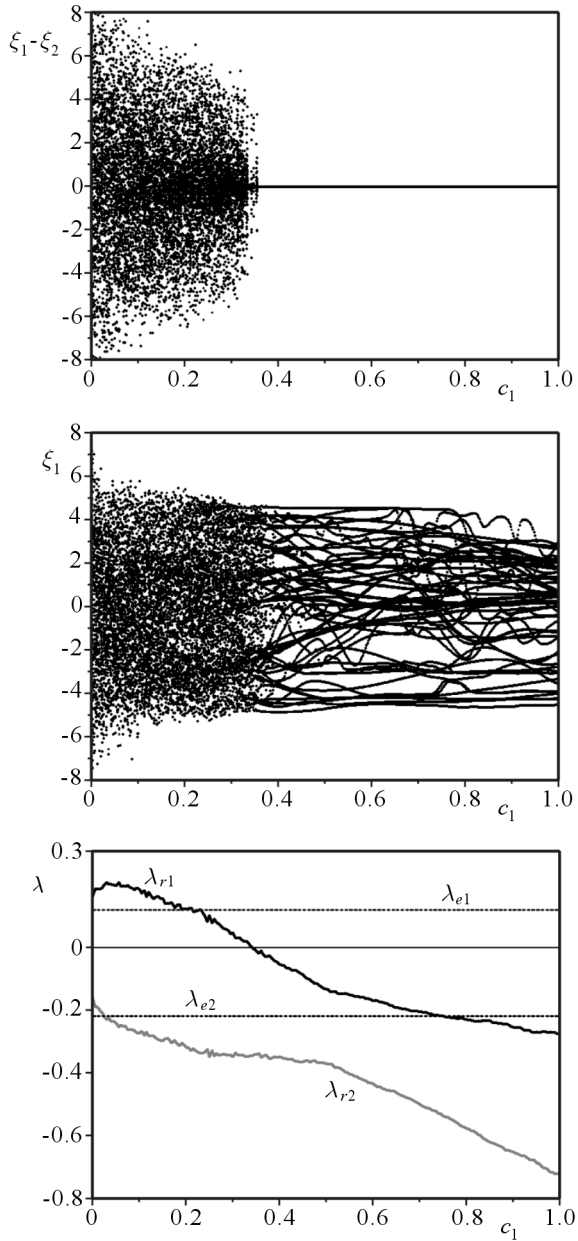


Fig. 9. Non-linear excitation – chaotic behaviour ($q = 5.6$), bifurcation diagrams of $\xi_1 - \xi_2$, ξ_1 and Lyapunov exponents

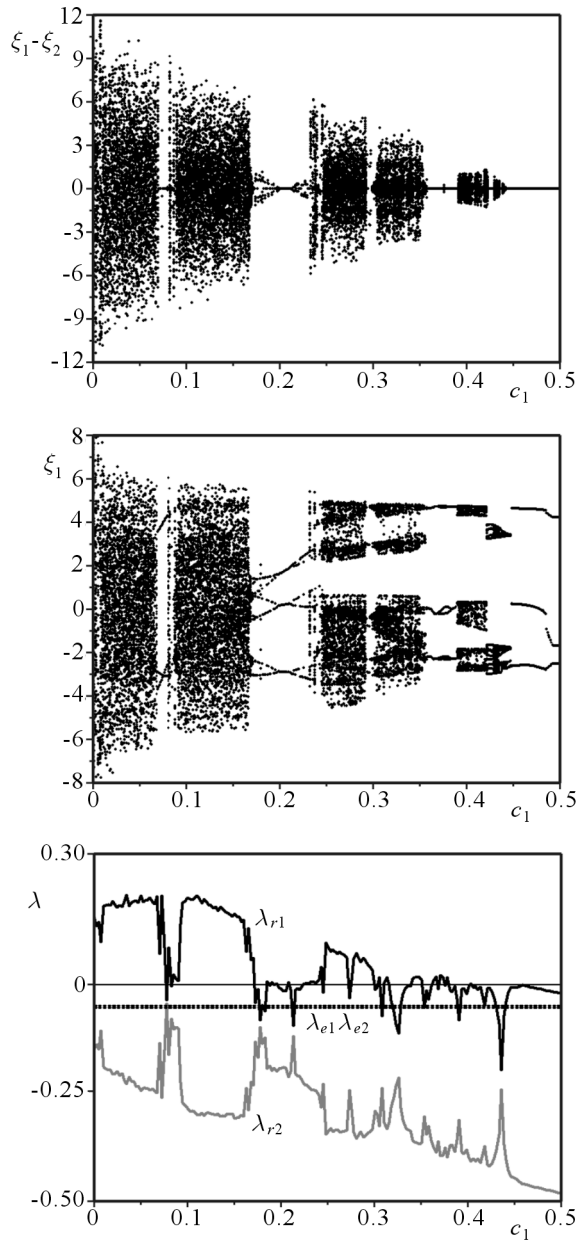


Fig. 10. Non-linear excitation – period three ($q = 5.8$), bifurcation diagrams of $\xi_1 - \xi_2$, ξ_1 and Lyapunov exponents

so on. The relation between the largest RLE and synchronization phenomena is confirmed. In Fig. 9, the synchronization is reached despite chaotic motion – in this way the oscillators lose their sensitivity to the initial conditions. It is possible because the phenomena of mode locking with the signal of excitation occur (it is proved in the next Subsection and shown in Fig. 16c). Pioncaré maps of the system with chaotic excitation ($q = 5.6$) are presented in Fig. 11. In Fig. 11a a map before synchronization range ($c_1 = 0.3$) where hyperchaos exists (two positive LEs – λ_{r1} and λ_{e1}) is shown. Figure 11b concerns the system working in the synchronous regime ($c_1 = 0.5$) and the chaotic attractor can be seen (mode locking regime with excitation occurs and only one LE is positive: λ_{e1}). In Fig. 11 a comparison of Pioncaré maps of excitation (grey color) and the response (black color) is shown. As can be seen, the transition from hyperchaos to chaos is exhibited by noticeable reduction of the fractal dimension from $D_{KY} = 2.76$ (Fig. 11a – hyperchaos) to $D_{KY} = 1.89$ (Fig. 11b – chaos).

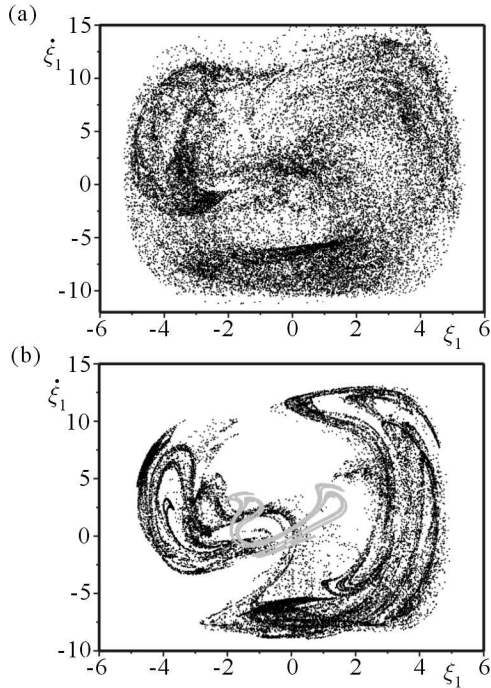


Fig. 11. Pioncaré maps of one subsystem excited by the chaotic signal (black dots) and a comparison map of the excitation (grey dots): (a) $c_1 = 0.3$ and $D_{KY} = 2.76$ (before synchronization), (b) $c_1 = 0.5$, $D_{KY} = 1.89$ (after synchronization)

In the last Figure in this subsection, the influence of perturbation on the stability of the synchronous state is shown. Every 50 periods of the driving system, the response systems have been perturbed by a small displacement ($\delta = 0.1$). After a short time, the response systems reach synchronization, which means that this state is stable.

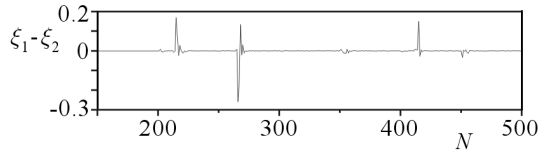


Fig. 12. Synchronization error $\xi_1 - \xi_2$ for $c_1 = 0.4$ and $q = 5.6$, after every 50 periods of the excitation signal, a small perturbation is added to the system

4.3. Coupled oscillators

Synchronization between forced coupled Duffing oscillators has been investigated in Perlikowski and Stefański (2006), Stefański and Kapitaniak (2003), Stefański *et al.* (2007). In this Section, two coupled Duffing oscillators excited kinematically, described by Eqs. (3.4), are taken under consideration. The excitation signal is given by the forced Duffing oscillator introduced in the previous Section. In these simulations, only one value of the parameter q : $q = 5.6$ (chaotic motion) has been used. The results of different kinds of analysis of the synchronization process in the examined system, are presented below.

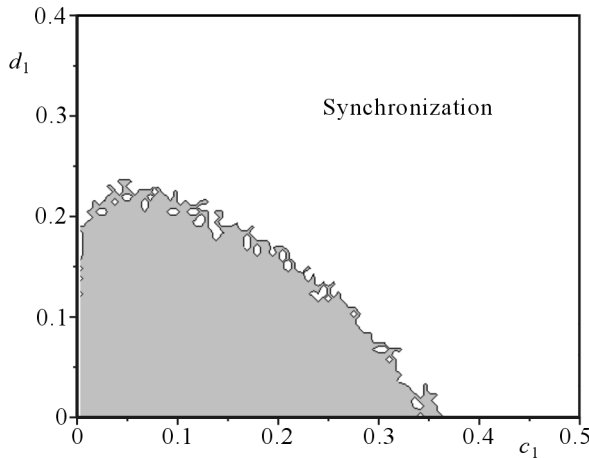


Fig. 13. Plot of the synchronization error $\xi_1 - \xi_2$ as a function of c_1 and d_1

In Fig. 13, a plot of the evolution of the synchronization error ($\epsilon = \xi_1 - \xi_2$) is shown. Then, in Fig. 14, values of RLE for the whole system presented in Fig. 5 are plotted. At the end (Fig. 15), the maximal TLE is presented. All figures exhibit the dependence on the dissipative parameters c_1 versus d_1 .

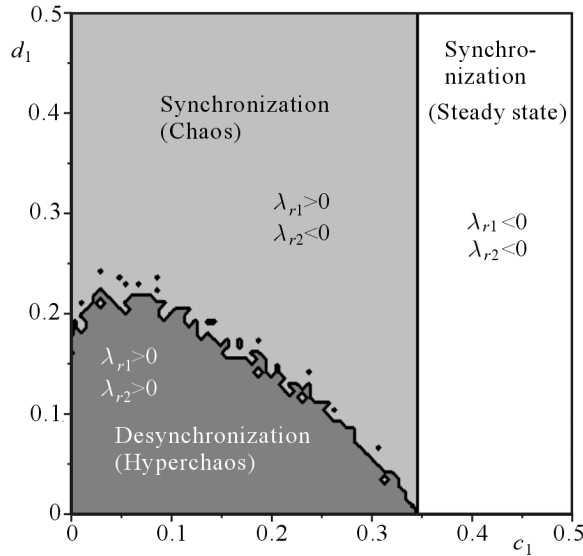


Fig. 14. Lyapunov exponents for the whole system for all cases: $\lambda_{r3} < 0$, $\lambda_{r4} < 0$, $\lambda_{e1} > 0$ and $\lambda_{e2} < 0$

The comparison of those three methods arises their interchangeability, but on the other hand, much more information about the system is possible to obtain by calculating LE. In Fig. 14 areas with three possible configurations of RLE are presented. The first range (dark grey) corresponds to desynchronization and hyperchaotic behaviour of the response systems. When the parameters are located in the light grey area, then the oscillators reach synchronization, but still there is no correlation with the signal of the excitation. In the last range (white), the oscillators not only synchronize but also the mode locking regime with the excitation occurs. In Fig. 16, phases for all cases are presented. Calculation of TLEs enabled one to present the synchronization area for any number of coupled oscillators and any set of coupling scheme, but in spite of RLE, less information about the system is attained.

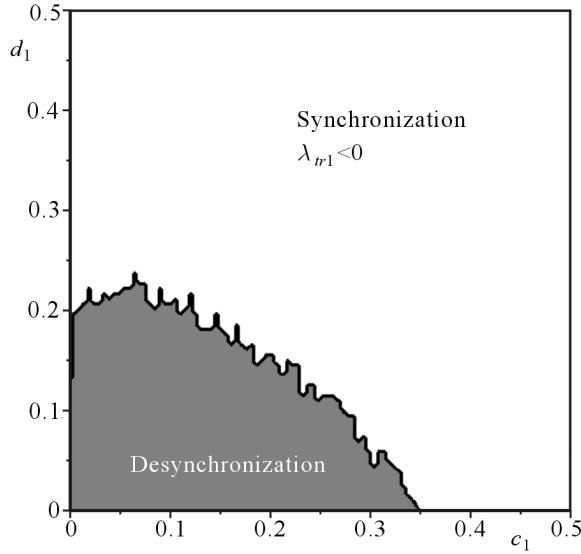


Fig. 15. Transversal Lyapunov exponents for all cases: $\lambda_{tr2} < 0$, $\lambda_{e1} > 0$ and $\lambda_{e2} < 0$

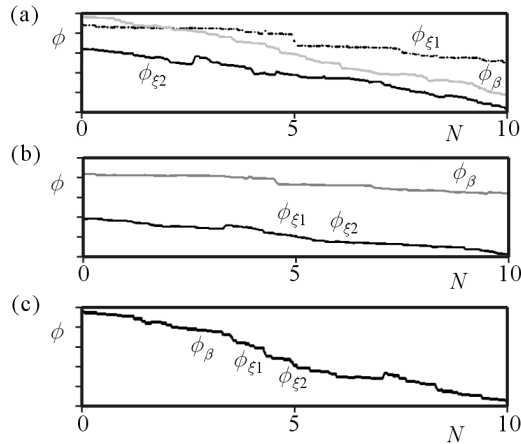


Fig. 16. Phase ϕ_{ξ_1} , ϕ_{ξ_2} , ϕ_{β} of the first and the second oscillator as well as the excitation, respectively; (a) hyperchaos for $c_1 = 0.1$, $d_1 = 0.1$, $d_2 = 0.0$, (b) chaos for $c_1 = 0.1$, $d_1 = 0.5$, $d_2 = 0.0$ and (c) steady state (mode locking) for $c_1 = 0.5$, $d_1 = 0.0$, $d_2 = 0.0$

5. Conclusion

In this work, phenomena of synchronization of mechanical oscillators excited by a common signal, also introduced by a mechanical system, have been shown. As a result, detection methods of synchronization in coupled and uncoupled

oscillators have been presented. The dependence on changes in the spectrum of Lyapunov exponents has also been investigated. It is worth mentioning that the period of the forced system tends to the period of the excitation. Whenever in the case of chaotic excitation, the response tends to the chaotic behaviour. It has been also found that uncoupled oscillators completely synchronize with each other when the mode locking regime with the excitation takes place. This phenomenon depends only on the inner viscous damping and is independent of dissipative connections between the oscillators. It is sufficient to calculate the spectrum of Lyapunov exponents of the single system to detect it.

Acknowledgment

This study has been supported by Polish Department for Scientific Research (DBN) under Project N501 044 31/2919.

References

1. BLEKHMEN I., LANDA P.S., ROSENBLUM M.G, 1995, Synchronization and chaotization in interacting dynamical systems, *Applied Mechanics Review*, **48**, 733-752
2. BOCCALETTI S., KURTHS J., OSIPOV G., VALLADARES D., ZHOU C., 2002, The synchronization of chaotic systems, *Physics Reports*, **366**
3. GABOR D., 1946, Theory of Communication, *J. IEE*, **93**, 429-457
4. KAPITANIAK T., 1994, Synchronization of chaos using continuous control, *Physical Review E*, **50**, 1642-1644
5. KAPITANIAK T., SEKIETA M., OGORZALEK M., 1996, Monotone synchronization of chaos, *International Journal of Bifurcation and Chaos*, **6**, 211-217
6. PARKER T., CHUA L., 1989, *Practical Numerical Algorithms for Chaotic Systems*, Springer-Verlag, New York
7. PECORA L., CARROLL T., 1990 Synchronization of chaotic systems, *Physical Review Letters*, **64**, 821-824
8. PECORA L., CARROLL T., 1991, Driving systems with chaotic signal, *Physical Review A*, **44**, 2374-2377
9. PECORA L., CARROLL T., 1998, Master stability functions for synchronized coupled systems, *Physical Review Letters*, **80**, 2109-2112
10. PERLIKOWSKI P., STEFAŃSKI A., 2006, Synchronization of coupled mechanical oscillators, *Mechanics and Mechanical Engineering*, **10**, 110-116

11. PYRAGAS K., 1993, Predictable chaos in slightly perturbed unpredictable chaotic systems, *Physics Letters A*, **181**, 203-210
12. ROSENBLUM M.G., PIKOVSKY A.S., KURTHS J., 1996, Phase synchronization of chaotic oscillators, *Physical Review Letters*, **76**, 1804-1807
13. ROSENBLUM M.G., PIKOVSKY A.S., KURTHS J., SCHAEFER C., TASS P., 2001, Phase synchronization: from theory to data analysis, *Handbook of Biological Physics*, **4**, 279-321
14. STEFAŃSKI A., KAPITANIAK T., 1996, Steady state locking in coupled chaotic systems, *Physics Letters A*, **210**, 279-282
15. STEFAŃSKI A., KAPITANIAK T., 2003a, Synchronization of mechanical systems driven by chaotic or random excitation, *Journal of Sound and Vibration*, **260**, 565-575
16. STEFAŃSKI A., KAPITANIAK T., 2003b, Synchronization of two chaotic oscillators via negative feedback mechanism, *Int. Journal of Solids and Structures*, **40**, 5175-5185
17. STEFAŃSKI A., PERLIKOWSKI P., KAPITANIAK T., 2006, Rugged synchronizability of coupled oscillators, *Physical Review E*, **75**

Synchronizacja oscylatorów mechanicznych wymuszanych kinematycznie

Streszczenie

W artykule pokazano numeryczną analizę dynamiki sprzężonych oscylatorów mechanicznych wymuszonych kinematycznie. Przedstawiono przegląd najważniejszych metod detekcji synchronizacji, zwracając szczególną uwagę na ich własności. Następnie opisano powiązania między widmem wykładników Lapunowa, a różnymi typami synchronizacji. Zbadano odpowiedź układu dla różnych typów sygnału wymuszającego (harmonicznego, okresowego i chaotycznego). Udowodniono, że zamykanie modów pomiędzy sygnałem oscylatora a wymuszeniem zależne jest tylko od tłumienia wewnętrzznego oscylatorów, natomiast jest niezależne od sprzężeń pomiędzy nimi.

Manuscript received April 23, 2007; accepted for print October 4, 2007